

Interim report: Dissipation Learning in Active Matter

Nhat Pham

School of Physics, University of Bristol

The first section aims to address generalities surrounding the studies of active matter, providing motivations from both practical and theoretical domains. The second section provides an overview of existing models in the field, what they are and how they compare to one another. The third and final section aims to detail progress made up to now, a discussion on the results from this preparatory work, and consequently a goal and plan for how the project will proceed going forward.

I. INTRODUCTION

An active matter system is characterised by its constituents undergoing active motion, which is caused by some internal self-propelling and self-directional mechanisms. The special characteristic of active motion is the capability to extract and dissipate energy, with dissipation the breaking of detailed balance that gives rise to irreversibility and non-equilibrium [1]. The cause of these mechanisms can range from specific biological activities to more general non-equilibrium dynamics [2], and the results of which are complex, systematic behaviours [3]. Numerous examples of active systems can be found in biological systems at all scales, from fish in a school [4] and birds in a flock, to algae, bacteria, proteins [5] and actin and microtubules in subcellular domains [3]. The general and intriguing features of active systems are often large-scale emergent collective phenomena, such as clustering, synchronous dynamics [5], order-disorder transitions [6], pattern formation [2], swarming, and lots more.

A. Real-world implications

We can connect tools and knowledge of active matter systems to practical applications, where we might want to borrow or mimic strategies from biological systems, with the goal of creating new synthetic materials, devices, robotics and medicine [7], as well as experimental techniques, such as automated digital tracking [2]. Here, models of active matter is an integral tool to provide insight and predictions. For this, the models are performed both *in vitro* (nanomachines) and *in silico* (numerical modelling). An overview of the latter can be found in Section II. Although active systems have a parameter space far from minimal, by using appropriate approximations to form our models, even with minimal ones, we can seek to derive large-scale generality [3, 8]. These systems have group-level properties derived from macroscopic orders, phases, and phase transitions, that are independent of the scale of its constituents.

For instance, a good yet minimal approximation would be a model by Viscek *et. al.* [6, 9]. Here, clustering is induced through a combination of self-propulsion and self-orientation in response to its neighbours. The system evolves with a two-step iteration process, and the whole system is controlled by 3 parameters. Yet, its cen-

tral prediction shows phase transition from disordered, individual motion to ordered, collective motion, dictated through its minimal set of parameters [6].

While it cannot be assumed that the models used *in vitro* translate directly to what is observed in reality, they are still crucial components that when combined with more sophisticated rules or understanding from other fields, would enable useful real-world applications, an example being controlling insect pest outbreaks [6].

B. New physics at non-equilibrium

Non-equilibrium regimes are ubiquitous in a biological world, yet they are not well-understood in physical theories. Non-equilibrium results when energy exchanges and dissipation at the level of individual particles' contribution lead to irreversibility within [7, 10]. This is contrasted with at-equilibrium systems, where energy effects are found at the system's boundaries [3]. Whereas we have the laws of thermodynamics and statistical mechanics in the latter type of systems that tell us about their macrostates (from their energy) and likelihood (from their Boltzmann distribution), it is not clear for the former type of systems. The difficulty lies in constructing analogues to these theories using quantities equivalent to the system's free energies. With new theoretical analogues, we can gain new ways of understanding this regime.

In addition to the bottom-up study of non-equilibrium behaviours by putting various models with determined individual dynamics to test to describe emergent collective behaviours, one challenge is to address the inverse problem; to determine the structural rules that lead to a desired collective state [11]. In this domain, powerful tools like machine learning can be deployed to connect activity with structure (expanded in Section III). With the ability to control and quantify both, we might be able to build a robust framework analogous to equilibrium statistical thermodynamics, but one which ultimately can provide fundamental (or at least more generalized) insight into microscopic-emergent connections [12]. The possibility and robustness of such a generalization of dynamical features is already hinted at by the vast and continuously increasing body of publications around these systems, despite the heterogeneous nature of individual units, from subcellular motors to desert locusts [2].

II. METHODOLOGY AND CONCEPTS IN THE MODELLING OF ACTIVE MATTER

Active matter models can be classified into either “dry” or “wet” models, where the latter considers the former’s particles with the addition of a solvent, whereas the former is limited to its equations of motion. While the use of dry models is to model real “dry” systems, they can be used as minimal systems where the solvent is only treated as a thermal bath (the cause of random fluctuations) [13]. Where these models are concerned, with emphasis on individual dynamics, the presence of random fluctuations amongst individual units is central to the modelling of these systems. While there may be different mechanisms to introduce randomness, functionally, it is possible to introduce these fluctuations stochastically by imbuing it directly in the dynamics and equations of motion of each individual unit [2]. This introduces the concept of active Brownian particles (ABP), which forms a class of systems that behave like Brownian particles (passive stochastic collisions, i.e. the thermal bath, which are typically passive colloids orders of magnitude smaller than the particles of the system [13]), but instead generalized to non-equilibrium regimes. In other words, these particles (normally modelled as spheres, but also as rods [14]) undergo repulsive self-propelled motion with overdamped dissipative dynamics [15], where dissipation dominates over inertial effects [13, 16].

In simple ABP models, the system can be controlled by two parameters, density ϕ , and the ratio of persistence length l_0 to particle size σ [17]. Overall, ABP has been quantitatively found to deviate from mere passive systems at individual-level dynamics (e.g., diffusion) in their stationary velocity and speed distributions [18] as well as by exhibiting at collective-level a phenomenon called motility-induced phase separation (MIPS) [13]. This exotic behaviour is found uniquely in non-equilibrium systems, where there is distinctive phase transition for liquid-gas at low activity as well as an ordered transition to crystallization at increasing activity and densely packed regimes [17].

In addition to ABP, there is a variety of alternatives: there is the run-and-tumble (RTP) model, which is characteristic of certain bacteria like *E. coli* [13, 19, 20], where MIPS has also been observed [21]. At coarse-grained scales and single-particle scale, RTP and ABP models show strict equivalence in some cases, with overall minor differences [21]. There is also the active Ornstein-Uhlenbeck particle (AOUP) model, where self-propulsion is generated by coloured Gaussian noise (time-correlated noise with a well-defined characteristic time at the scale of the system itself [16]). At large scales, MIPS is observed [22], but the model diverges significantly at single-particle level when compared to ABP and RTP [13].

Besides particle-based models, there exist numerous field-based, or continuum theories, which are constructed using PDEs for parameter fields that are stochastic and active by removing them from field-based constraints of

time-reversal symmetry (constraints involving the existence of free energy, the Boltzmann distribution, steady states, etc. [1]). Overall, a continuum theory can be constructed bottom-up by coarse-graining microscopic details, or top-down by imposing symmetry and conservation laws on the equations, with noise added. While these are mostly general models in the sense they do not require specific mechanisms, continuum theories can generate phenomenological models for specific cases, such as in bacterial turbulence. Otherwise, they are deployed to also explicitly account for hydrodynamical (or “wet”) interactions at low density [13].

A. Discrete, lattice-based models

While off-lattice (continuous) models provide an edge when the studies concerned are phenomenological, such as the run-and-tumble strategies of *E. coli* and other bacteria. However, for more fundamental studies of general non-equilibrium physics, lattice models are appropriate tools, as they are computationally cheaper, and easier to extend to higher dimensions [20] when compared to off-lattice models, which are not as efficient when particle interactions are involved. For lattice models, implemented with discrete timesteps, interactions concerning hopping from site to site can be characterised in a number of different ways. One very simple way is to implement a zero-range interaction, or process (ZRP), where the rate of a given particle to hop from its departure site to one of its direct-neighbours is a function of the total number of particles at the departure site. There is no dependence on the arrival site [20].

This is contrasted with exclusion processes, where the rate of hopping depends on occupation of the arrival site, where occupation is defined as having a certain maximum number of particles. If the destination is occupied, the particle remains at its departure site until it either orients away or the arrival site becomes free [20, 23]. Our model implements an exclusion process.

B. An overview on persistent exclusion process

The persistent exclusion process (PEP) model is lattice-based (see II A), with run-and-tumble dynamics (see Section II), where persistent motion (the inverse of the tumbling rate, α , for a particle to “tumble”, i.e. randomise its direction) characterises non-equilibrium behaviour [19, 20]. In such model, its robustness is controlled by the lattice size, (or density ϕ), as well as α . In our version of PEP (as well as in [19, 24]), the lattice is a two-dimensional realization with size $L_x \times L_y$, measured in lattice sizes. Naturally, this gives total number of particles $N = \phi L_x L_y$. For each particle, an orientation \mathbf{s} dictates the direction to which it points. In each iteration (time evolves in a discrete manner), each particle either remains in its ‘run’ state, and moves to the neigh-

bour it points at if the site is vacant, or in the case where it undergoes a tumble, it changes its orientation to a new s' , which is drawn at random and independent of the original value [24]. To impose particle exclusion (or excluded volume), each lattice site has maximum occupancy, and thus aggregation, or clustering, is seen to happen when two particles “jam” (collide head-first) in the single-occupancy case. When jammed, particles create a cluster seed. Besides cluster formation, there are various significant cluster dynamics to note (in non-equilibrium conditions, i.e. when $\alpha \neq 1$): absorption of particles at cluster boundaries, where particles get stopped by existing clusters, and evaporation of particles at cluster boundaries, where particles tumble to point away from clusters and leave.

There are three characteristic timescales to consider: first, the ‘update time’, or the time it takes for a particle to cross a site τ . Second, the mean ‘flight time’ [24], which is the mean time spent in the run state [25], and finally, the timescale of α^{-1} , which ought to be compared to the first two. Tumbling duration is assumed to be instantaneous in this model.

III. PROGRESS, DISCUSSION, AND PLANS

A. Current work and discussion

Over the initial 7 weeks of the project, we have worked through the in-house code package [26] (referred to as the PEP code here onwards), annotating and documenting what it does step by step. The code is a Python implementation (with `ctypes`) of the PEP process (see Section II B). In short, it is a stochastic, lattice implementation where every particle has 4 isotropic degrees of freedom (up, down, left, right), similar to what is described in [19]. The PEP code was validated and tested at a range of values for each of α and ϕ . Specifically, α was chosen to be within the range 2^n , $n \in [-6 \dots -1]$, and ϕ was chosen to be within the range $0.05m$, $m \in [1 \dots 10]$. At each step, all particles are updated in random order, where each particle attempts to move to their destination, and then has a chance of tumbling. Cluster formation was seen to occur, as seen in Fig. 1; here it is clear that after 20 timesteps, the system evolved from homogeneity to small groups of cluster, and after 200 timesteps, a percolation transition can be seen to have taken place. Clusters are smaller and more spread out at $\tau = 0$, compared to $\tau = 200$, where clusters are much bigger and form networks. Here, steady-state is observed, with constant evaporation happening at cluster borders, but also constant clusters formation that maintain the overall percolation appearance.

Two characteristics have been measured: the cluster size distributions, and the number of cluster, all at different values of (ϕ, α) . Cluster size distributions, as seen in Fig. 2 seem to mirror the appearance in [19] (fitting ought to be performed to validate the results seen in the afore-

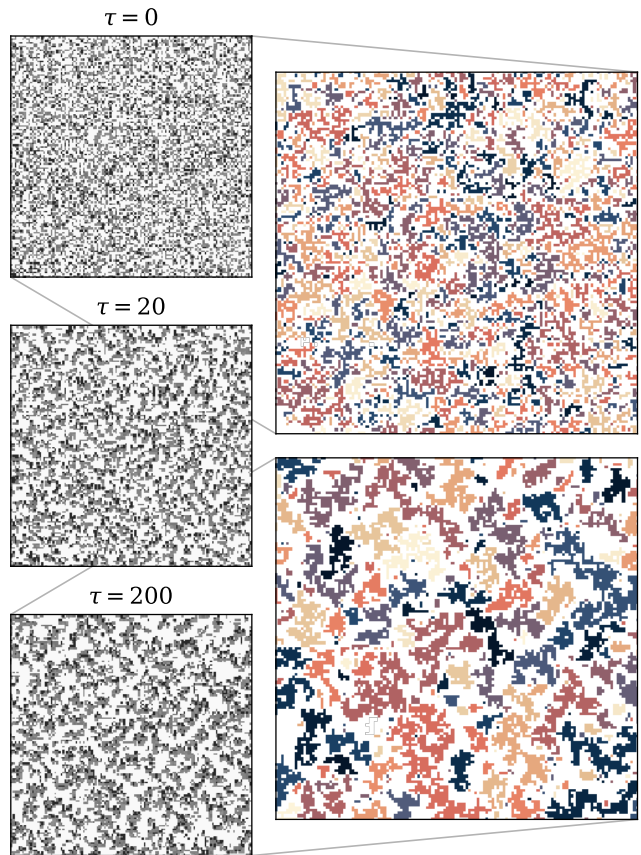


FIG. 1. Greyscale panels show system evolution at three distinct timesteps: $\tau \in \{0, 20, 200\}$, starting from top to bottom. Different shades of grey represent particle orientation. The coloured panels show labelled clusters, using `scipy.ndimage()`, for $\tau = 0$ (top) and $\tau = 200$ (bottom). Particle connections are established for neighbours in the up, down, left, right directions. For this system, $\alpha = 0.023$, and $\phi = 0.45$.

mentioned work). Nonetheless, the cluster sizes do seem to correspond well to expected behaviour: larger clusters are observed only at higher densities, with the largest sizes exclusive to systems that display percolation transition (as seen in the top and middle right panel). The middle column ($\phi = 0.25$) displays the clearest effects of α on cluster formation. Higher α corresponds to more frequent tumbles (and lower persistence times), and thus interaction looks closer to the equilibrium case of passive Brownian particles, where local densities are more homogeneous (in fact, the equilibrium limit is $\alpha = 0$). Below certain thresholds of (ϕ, α) , particle concentration is sufficiently low to not display any steady-state at all. These thresholds ought to be determined, and restrict our systems to values above such thresholds.

For this, we can look to the number of clusters, as seen in Fig. 3, where the behaviour also appears to be as expected. The number of clusters increases as α increases, with the exception of the lowest density, $\phi = 0.05$, where

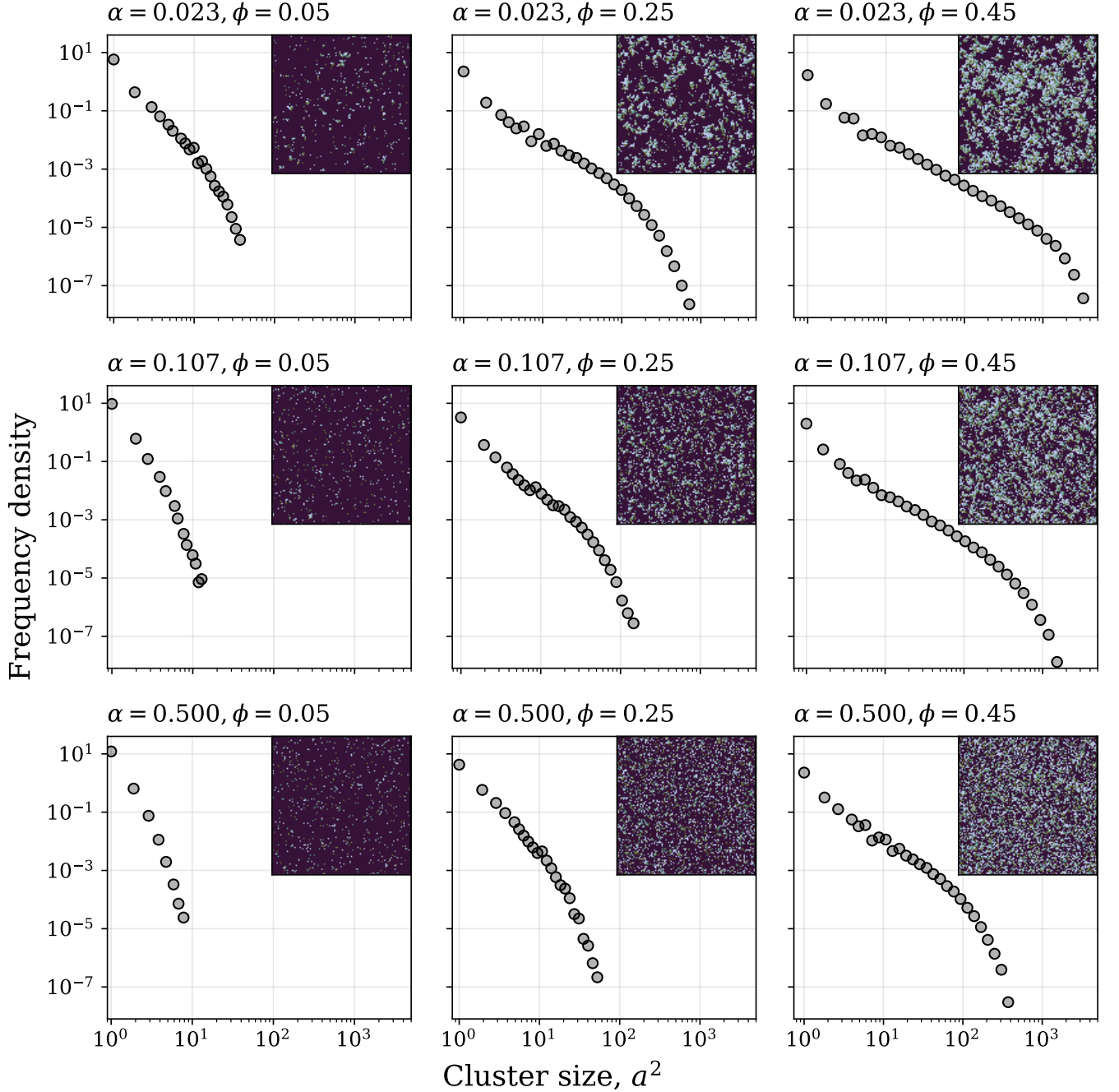


FIG. 2. The distribution of cluster sizes for a variety of α and ϕ . Density increases row-wise, from left to right, with $\phi = \{0.05, 0.25, 0.45\}$. Tumbling rate increases column-wise, from top to bottom, with $\alpha = \{0.023, 0.107, 0.500\}$. The symbol represents the frequency density at each cluster size bin, with logarithmic bins, counted over 1000 iterations post-steady-state. The inset for each pair of (ϕ, α) shows the snapshot of the 1000th iteration, where the dark colour is the background and shades of teal correspond to particles with different orientation.

it looks almost uniform (more data would be needed to confirm). This is expected as at such low concentrations, increasing tumbling might increase the rate at which clusters form, but clusters don't necessarily absorb more as there are so few particles around, thus clusters are likely to be more ephemeral as the centre of the clusters are

not trapped by its boundaries, so can freely move away. What is also expected is that a higher ϕ would give more clusters, but above a certain threshold of ϕ , tight packing and percolation starts happening and clusters become big and fewer in number. This is seen when contrasting between $\phi = 0.25$ and $\phi = 0.45$. Overall, more data

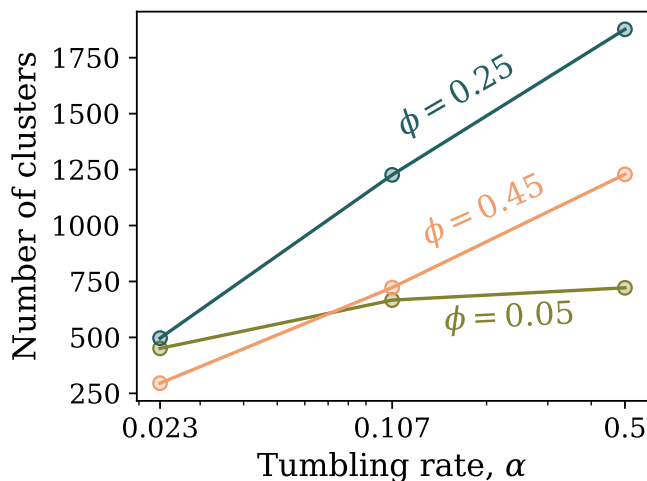


FIG. 3. The number of distinct clusters identified (where distinction is made separated by having neighbours not directly up, down, left, or right) as tumbling rate α increases. Each solid line represents a different density, with three values, $\phi = \{0.05, 0.25, 0.45\}$ shown here. Here, the number of clusters is averaged over 1000 iterations for each data point (represented as symbols), with the distance between successive iteration scaled with α^{-1} .

ought to improve this characterisation; we expect to find a threshold ϕ for which the number of clusters start to decrease, and the range of α for which this is seen.

We have identified other characterisations to potentially implement (as additional asides to investigate): we could look to particle orientation and cluster seed formation (head-on collisions) over time. The strategy for the former would be to look at the frequency of a given orientation over time (instead of the system's mean orientation). For the latter, the simplest implementation would be to track the number of aborted move attempts during data sampling. In addition to this, the pair correlation function (or radial distribution function, which, for a particle, describes particle density as a function of radial distance) could be implemented to add to the overall structural characterisation. In brief, beyond these few additional things to look into, so far, the model was updated and revised at places, and the important char-

acterisations were implemented, and looks to correspond well with [19].

B. Goals and plans

The goal, ultimately, is to train a convolution neural network to identify dissipation, which we take here to be defined as the ratio between the mass transfer time and the diffusion time, i.e. Péclet number, P_E . This relates to the speed, v , the diffusion coefficient $D = \alpha^{-1}$ [19], and the interaction range σ [12], which is unity. This gives $P_E = v\alpha$ [27]. This has previously been done in [12]: using a convolutional neural network (CNN), the static structural configuration of an AOUP system (taken to be the pair correlations) was linked to dissipation (which was taken to be the active work per particle), without any knowledge of the underlying dynamics. It is our goal to bring this onto a lattice-based PEP implementation, where static structural configuration can be single snapshots of cluster properties and distribution, with and without orientation characterisations, and see if dissipation in terms of P_E can be linked. We will implement this in Keras (Tensorflow), and the plan is to tune the neural network to get a configuration that is not too computationally expensive, using minimal data, but able to retain accuracy (using pair correlations and other features we implement) and some robustness (beyond the standard variations in α and ϕ). This means devising pipelines to test how well it can scale (up or down), does it work before the system enters steady-state, and does it work if we tweak the models (for different exclusion thresholds, different persistence mechanics to RTP).

From this, the next steps would be to get to grips with CNNs and finesse our in-house code to have all the characterisations to prepare the dataset for training, before we can start implementing a simple model with minimal layers for the CNN. Then, we can proceed to evaluating the model, at this stage, if good predictions for dissipation are obtained, we can look into trying out different layers, optimizers and other features in order better accuracy, as well as build novel situations to test and increase robustness.

[1] M. E. Cates, enActive Field Theories (2019), arXiv:1904.01330 [cond-mat].
[2] P. Romanczuk, M. Bär, W. Ebeling, B. Lindner, and L. Schimansky-Geier, enActive Brownian particles, The European Physical Journal Special Topics **202**, 1 (2012).
[3] M. C. Marchetti, J. F. Joanny, S. Ramaswamy, T. B. Liverpool, J. Prost, M. Rao, and R. A. Simha, Hydrodynamics of soft active matter, Reviews of Modern Physics **85**, 1143 (2013), publisher: American Physical Society.
[4] Y. Yang, F. Turci, E. Kague, C. L. Hammond, J. Russo, and C. P. Royall, enDominating lengthscales of zebrafish

collective behaviour, PLOS Computational Biology **18**, e1009394 (2022), publisher: Public Library of Science.
[5] S. Decamp, enWhat is Active Matter?
[6] J. Buhl, D. J. T. Sumpter, I. D. Couzin, J. J. Hale, E. Despland, E. R. Miller, and S. J. Simpson, From Disorder to Order in Marching Locusts, Science **312**, 1402 (2006), publisher: American Association for the Advancement of Science.
[7] C. Bechinger, R. Di Leonardo, H. Löwen, C. Reichhardt, G. Volpe, and G. Volpe, enActive Particles in Complex and Crowded Environments, Reviews of Modern Physics

- 88**, 045006 (2016).
- [8] E. Flenner and G. Szamel, Active matter: quantifying the departure from equilibrium, *Physical Review E* **102**, 022607 (2020), arXiv:2004.11925 [cond-mat].
 - [9] T. Vicsek, A. Czirók, E. Ben-Jacob, I. Cohen, and O. Shochet, enNovel Type of Phase Transition in a System of Self-Driven Particles, **75**, 1226 (1995).
 - [10] S. Ramaswamy, enThe Mechanics and Statistics of Active Matter, *Annual Review of Condensed Matter Physics* **1**, 323 (2010).
 - [11] G. Gompper, R. G. Winkler, T. Speck, A. Solon, C. Nardini, F. Peruani, H. Löwen, R. Golestanian, U. B. Kaupp, L. Alvarez, T. Kiørboe, E. Lauga, W. C. K. Poon, A. DeSimone, S. Muiños-Landin, A. Fischer, N. A. Söker, F. Cichos, R. Kapral, P. Gaspard, M. Ripoll, F. Sagues, A. Doostmohammadi, J. M. Yeomans, I. S. Aranson, C. Bechinger, H. Stark, C. K. Hemelrijk, F. J. Nedelec, T. Sarkar, T. Aryaksama, M. Lacroix, G. Duclos, V. Yashunsky, P. Silberzan, M. Arroyo, and S. Kale, enThe 2020 motile active matter roadmap, *Journal of Physics: Condensed Matter* **32**, 193001 (2020).
 - [12] G. Rassolov, L. Tociu, Fodor, and S. Vaikuntanathan, enFrom predicting to learning dissipation from pair correlations of active liquids, *The Journal of Chemical Physics* **157**, 054901 (2022).
 - [13] L. Hecht, J. C. Ureña, and B. Liebchen, *An Introduction to Modeling Approaches of Active Matter* (2021).
 - [14] F. Peruani, A. Deutsch, and M. Bär, Nonequilibrium clustering of self-propelled rods, *Physical Review E* **74**, 030904 (2006), publisher: American Physical Society.
 - [15] M. C. Marchetti, Y. Fily, S. Henkes, A. Patch, and D. Yllanes, Minimal model of active colloids highlights the role of mechanical interactions in controlling the emergent behavior of active matter, *Current Opinion in Colloid & Interface Science* **21**, 34 (2016), arXiv:1510.00425 [cond-mat].
 - [16] P. Häunggi and P. Jung, EnglishColored Noise in Dynamical Systems (2007) pp. 239–326, qID: Q99980034.
 - [17] A. K. Omar, K. Klymko, T. GrandPre, and P. L. Geissler, enPhase Diagram of Active Brownian Spheres: Crystallization and the Metastability of Motility-Induced Phase Separation, *Physical Review Letters* **126**, 188002 (2021).
 - [18] P. Romanczuk and L. Schimansky-Geier, enBrownian Motion with Active Fluctuations, *Physical Review Letters* **106**, 230601 (2011).
 - [19] R. Soto and R. Golestanian, enRun-and-tumble dynamics in a crowded environment: Persistent exclusion process for swimmers, *Physical Review E* **89**, 012706 (2014).
 - [20] A. G. Thompson, J. Tailleur, M. E. Cates, and R. A. Blythe, enLattice models of nonequilibrium bacterial dynamics, *Journal of Statistical Mechanics: Theory and Experiment* **2011**, P02029 (2011).
 - [21] M. E. Cates and J. Tailleur, enWhen are active Brownian particles and run-and-tumble particles equivalent? Consequences for motility-induced phase separation, *Europhysics Letters* **101**, 20010 (2013), publisher: EDP Sciences, IOP Publishing and Società Italiana di Fisica.
 - [22] Fodor, C. Nardini, M. E. Cates, J. Tailleur, P. Visco, and F. Van Wijland, enHow Far from Equilibrium Is Active Matter?, *Physical Review Letters* **117**, 038103 (2016).
 - [23] S. Zhang, A. Chong, and B. D. Hughes, engPersistent exclusion processes: Inertia, drift, mixing, and correlation, *Physical Review E* **100**, 042415 (2019).
 - [24] N. Sepúlveda and R. Soto, enWetting Transitions Displayed by Persistent Active Particles, *Physical Review Letters* **119**, 078001 (2017).
 - [25] Is that right?
 - [26] Persistent Exclusion Process (2023), original-date: 2023-10-10T13:16:03Z.
 - [27] I don't know if this is correct.